International Journal of Power Electronics and Drive System (IJPEDS)
Vol. 17, No. 2, June 2026, pp. 1313~1325
ISSN: 2088-8694, DOI: 10.11591/ijpeds.v17.i2.pp1313-1325

Robust power optimization strategy for wind-driven induction machines using type-2 and type-1 fuzzy logic controllers

Driss Belkhiri[1], Boujemaa Nassiri[2], Mohamed Ajaamoum[1]
[1]Laboratory of Engineering Sciences and Energy Management, High School of Technology, Ibn Zohr University, Agadir, Morocco
[2]LSIAR Polytechnique School, International University of Agadir, Agadir, Morocco

Article Info

Article history:

Received May 16, 2025
Revised Feb 21, 2026
Accepted Mar 6, 2026

Keywords:

Advanced methods
Conventional methods
Intelligent control
Maximum power monitoring
Renewable energy
Wind energy systems

ABSTRACT

This paper proposes a reliable power optimization strategy that maximizes the harvested power of induction machines driven by wind, taking into account variable wind turbulence and uncertain machine parameters. This work explores the challenging task of designing type-2 fuzzy logic (T2FL) and conventional type-1 fuzzy logic (T1FL) controllers for wind energy conversion systems that exhibit multiple non-linearities. T2FL controllers are proficient in tackling uncertainties and offer quicker and more precise decision-making capabilities. The proposed approach is beneficial as it is independent of accurate wind turbine parameters, wind speed data, or additional sensors. Rather, it utilizes the mechanical rotor speed and the wind turbine power as input, which corresponds to maximum power point tracking (MPPT) through the management of the rotor speed via the machine-side converter. Real data validates the scheme against classical controllers, and via a set of simulations and statistical analyses, performance metrics like steady-state error, overshoot, tracking speed, and efficiency are widely assessed. The results show that the proposed scheme, which is independent of a dedicated wind speed sensor, demonstrates superior tracking performance, lower tracking errors, such as lower RMSE/MAE, and higher energy yield, although the wind speed and the system parameters change rapidly. Overall, this design provides more robust performance to random wind speed variations, increases operational efficiency and wind turbines' service life, and is low in adding mass and cost.

Corresponding Author:

Driss Belkhiri
Laboratory of Engineering Sciences and Energy Management, High School of Technology
Ibn Zohr University
Agadir, Morocco
Email: driss.belkhiri@edu.uiz.ac.ma

1. INTRODUCTION

The continuing increase in global energy requirements and increasing environmental issues, such as air pollution and climate change, have driven the shift towards sustainable and renewable sources of energy. Wind energy is considered one of the most promising candidates among them because of its technological maturity, decreasing costs in generating electricity, and its significant contribution to the reduction of greenhouse gas emissions [1], [2]. Consequently, the large-scale potential of wind energy system application is dispersing on the global level, contributing significantly to decarbonization and long-term energy security.

Modern wind power conversion systems are heavily dependent on advanced power electronic converters and control strategies to achieve efficient conversion of wind's kinetic energy to electrical power, reduced dependence on fossil fuels, and secure grid integration [3], [4]. However, the random and variable nature of wind resource still remains a problem to attain an optimal energy extraction, snap recovery for

system operation reliability, and improved overall system efficiency. These difficulties dictate the need for well-established control strategies and a tailored drive system to cope with varying system parameters, wind, and grid conditions [5].

To solve these problems, many advanced control strategies, such as maximum power point tracking (MPPT), have been used in order to maximize the energy captured under different circumstances. For large-scale wind energy conversion systems (WECS), instead of wind turbine generators with cage induction generator, doubly fed induction generator (DFIG) has been widely installed owing to its potential advantages, including being able to operate over a wide speed range and provide reactive power support for the grid and higher efficiency with relatively smaller converter capacity [6], [7]. These benefits result in the DFIG being a prominent technology for current generation wind farms, and additionally, they illustrate the significance of sophisticated control as well as power electronic aspects to ensure that its performance potential is fully capitalized upon.

In spite of the considerable benefits offered by DFIG-based WECS, the nonlinear characteristics of WECS, in addition to the stochastic and rapidly fluctuating behavior of wind speed, make it a hard task for MPPT [8]. Traditional MPPT algorithms such as the tip-speed-ratio method, optimal control of torque, power signal feedback control, and hill climb search [9]–[11] are popularly used in practice due to their simplicity and easy realization. Unfortunately, these methods are not satisfactory in tracking performance, dynamic response, or robustness against fast, high-frequency wind changes and disturbed operating points. These constraints not only decrease the extracted energy but may also cause unwanted oscillations, which greatly reduce system reliability and efficiency.

To address these disadvantages, a diverse set of intelligent control schemes, such as machine learning (ML) and neural networks (NN) [12]–[14], bio-inspired algorithms like genetic algorithms and particle swarm optimization [15], [16], and FLCs [17], have been introduced in recent years. Although these methods are promising in improving tracking accuracy, they are often bound by computational complexity, massive data for training, and convergence problems [7], [17] in real-time applications. Comparably, bio-inspired algorithms may suffer convergence and tunability problems [18], [19], thereby making them hardly applicable to WECS at large scales. There are also type-1 and type-2 FLC, which have been reported to be more robust and flexible in regulating nonlinear systems and thus considered as suitable models for WECS applications [20], [21].

Thus, there is still a strong demand for efficient, adaptive, and computationally effective MPPT techniques that can cope with practical non-linearities and uncertainties in DFIG-based systems. Previous studies have shown that FLCs have potential; for example, [22] reduced the converter size by 40% with a sensorless type-1 FLC for DFIG systems. As another example, [23] integrated NNs with type-1 FLC for enhancing power transfer response. While research studies involving permanent magnet synchronous generators (PMSGs) and adaptive FLCs [24]–[26] demonstrate promise, many of them lack rigorous experimental validation in real and uncertain environments. The adaptive FLC-based MPPT schemes for PMSG-based WESs have been proposed in [25], [27] with high efficiency and accuracy under simplified conditions such as the step or linear wind profiles. However, their performance in realistic scenarios, when wind speed will vary quickly, and system parameters become time-varying, has not been established yet, pointing out the necessity for robust adaptive optimizers for the non-linear and uncertain nature of the system.

In this context, a new MPPT control method of DFIG-based WECS based on IT2FLC is proposed in this study, by using a real wind profile and subjecting the system to parameter uncertainties, thus providing a more realistic and comprehensive validation. The proposed approach extends the established capabilities of type-1 FLCs by exploiting the superior uncertainty-handling properties introduced by IT2FLC to deal with parameter variations and nonlinearities present in wind energy systems. The primary contribution of this paper is its full experimental study of the IT2FLC-based MPPT with parameter uncertainties and varying wind profiles. The proposed FLC scheme is then investigated and compared with a traditional type-1 FL controller and an optimal torque controller (OTC), taking system nonlinearities, i.e., inertia, inductances, and resistance, quickly into account. The obtained results reveal that the approach of IT2FLC has shown better efficiency compared to the traditional T1FLC one, regarding robustness, tracking accuracy, and extraction power efficiency, which guarantees a real application solution for wind energy resources. The rest of the paper is structured as follows: i) Section 2 describes the model of the DFIG-based WECS; ii) Section 3 introduces the methodology employed to design the proposed controller; iii) Section 4 discusses the comparative performance via dynamic wind profiles; and v) Concluding remarks are noted in section 5.

2. SYSTEM CONFIGURATION OF WIND ENERGY CONVERSION SYSTEMS

Many classes of wind power generators have been presented for variable-speed WECS, and DFIGs are known for their high efficiency, low cost, and reliability [12], [26]. Figure 1 shows the overall system and

its MPPT scheme, which consists of the following subsystems: wind turbine (WT) (with three blades), gearbox & shaft, generator, and FLC scheme. The direct grid connection of DFIG is the stator, and the grid connection of the rotor winding is via a back-to-back converter, which is made up of a rotor side converter (RSC) and a grid side converter (GSC).

Basically, the wind turbine is the most critical component of WECS because it is responsible for converting the kinetic energy associated with the airstreams into mechanical energy. The mechanical power P_m generated by available wind speed V_w is expressed as (1).

$$P_m = \frac{1}{2}\rho S C_p(\lambda,\beta) V_w^3 \quad (1)$$

Where ρ represents the air density, S denotes the turbine sweeping area, λ is the tip-speed ratio (TSR), β is the pitch-angle, and the coefficient $C_p(\lambda,\beta)$ is a parameter with no dimensions that specifies how much the incoming wind power the WT can collect. It is determined by the WT's aerodynamics and can be expressed mathematically in relation to λ and β. The following equation can be used to approximate the expression of the C_p for this type of 1.5 MW DFIG wind turbine found in literature [28], [29].

$$C_p = (0.35 - ((0.00167(\beta-2)))\, sin(\frac{\pi(\lambda+0.1)}{(14.35-(0.3(\beta-2)))})) - (0.00184(\lambda-3)(\beta-2)) \quad (2)$$

Usually, the pitch angle β is set to 0 in order to harvest the maximum amount of energy feasible from the wind. Then, the factor C_p has a one-of-a-kind maximum point, which is C_p^{max} = 4.012 at λ = 8.2. Additionally, the tip-speed ratio λ is defined as (3).

$$\lambda = \frac{R\omega_m}{V_w} \quad (3)$$

The (3) is used to determine the reference rotor speed ω_m, which is denoted by (4).

$$\omega_m^* = \frac{\lambda_{opt} V_W}{R} \quad (4)$$

Hence, the maximal mechanical power harnessed by WT is expressed as (5).

$$P_m^{max} = \frac{\rho\, \pi\, R^5}{2\, \lambda_{opt}^{\,3}}\, V_w\, \omega_m^{*\,3}\, C_P^{max} \quad (5)$$

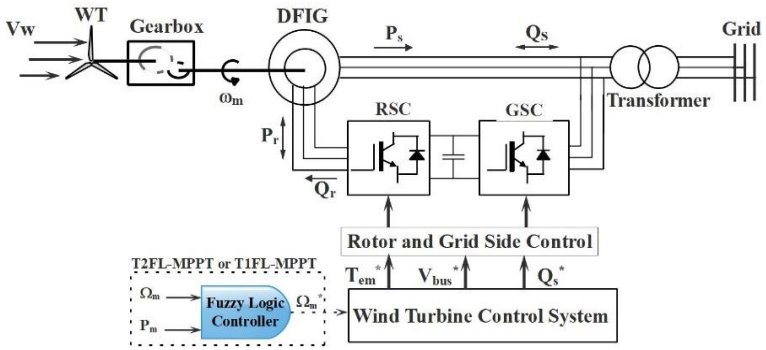

Figure 1. Simplified model of the WECS equipped with a DFIG-based wind turbine

2.1. Modeling of a doubly fed induction generator

In doubly fed asynchronous generator (DFIG) wind systems, the reference frame theory is used to make the study of electrical machines simpler. By applying the Park and Concordia transformation to the basic scheme of the DFIG in the three-phase (abc) frame, we derive the simplified dynamic equations of rotor and stator voltages in the synchronous framework (d, q) as (6) and (7).

$$\begin{cases} v_{dr} = R_r i_{dr} + \frac{d\psi_{dr}}{dt} - \omega_r \psi_{qr} \\ v_{qr} = R_r i_{qr} + \frac{d\psi_{qr}}{dt} + \omega_r \psi_{qr} \end{cases} \quad (6)$$

$$\begin{cases} v_{ds} = R_s i_{ds} + \frac{d\psi_{ds}}{dt} - \omega_s \psi_{qs} \\ v_{qs} = R_s i_{qs} + \frac{d\psi_{qs}}{dt} + \omega_s \psi_{ds} \end{cases} \quad (7)$$

Moreover, the flux linkages between the stator and rotor are specified as (8) and (9).

$$\begin{cases} \psi_{dr} = L_r i_{dr} + L_m i_{ds} \\ \psi_{qr} = L_r i_{qr} + L_m i_{qs} \end{cases} \quad (8)$$

$$\begin{cases} \psi_{ds} = L_s i_{ds} + L_m i_{dr} \\ \psi_{qs} = L_s i_{qs} + L_m i_{qr} \end{cases} \quad (9)$$

Usually, the relationship between the stator speed ωs and the angular frequency of the rotor ω_m is as (10).

$$\omega_r = \omega_s - \omega_m \quad (10)$$

Hence, the slip ring for rotor windings of the DFIG is given by (11).

$$s = \frac{\omega_s - \omega_m}{\omega_s} = 1 - \frac{p\Omega_m}{\omega_s} \quad (11)$$

Eventually, the difference in mechanical and electrical torque results in a variation in generator speed, which may be computed using (12) [9].

$$J\frac{d\Omega_m}{dt} = T_m(t) - T_e(t) \quad (12)$$

T_e denotes the generator's electric torque, which is given by (13).

$$T_e = \frac{3M}{2L_s} p\ (\psi_{qs} i_{dr} - \psi_{ds} i_{qr}) \quad (13)$$

By definition, the active and reactive powers through the stator and rotor can be expressed as (14) and (15).

$$\begin{cases} P_s = v_{ds} i_{ds} + v_{qs} i_{qs} \\ Q_s = v_{qs} i_{ds} - v_{ds} i_{qs} \end{cases} \quad (14)$$

$$\begin{cases} P_r = v_{dr} i_{dr} + v_{qr} i_{qr} \\ Q_r = v_{qr} i_{dr} - v_{dr} i_{qr} \end{cases} \quad (15)$$

When the resistance of the stator is neglected, i.e., $R_s = 0$ as introduced in [5]. The electric power of the generator P_e is given by (16).

$$P_e = P_s + P_r \quad (16)$$

In order to achieve safe, reliable, and efficient operation of WECSs, the FOC technique has become one of the most effective vector control tools for controlling wind generators [26]. The rotor speed, electromagnetic torque, and stator terminal power factor of the DFIG are controlled by the RSC. In that regard, the RSC is studied in this paper to compare the performance of the targeted type-2 and type-1 FL controllers. The electromagnetic torque and reactive power components can be separated by using the stator flux-oriented synchronous reference frame such that the d-axis is aligned with the stator flux vector, where axes rotate in accordance with synchronous speed. By this configuration, the stator voltage component along the q-axis is eliminated, so that it becomes possible to resolve three-phase rotor currents into real and reactive components independently controllable from each other.

3. MPPT CONTROL STRATEGY

The section describes the proposed MPPT technique developed for extracting efficient power from a wind energy system (WES) during different operating conditions. Figure 2 outlines the turbine's dual operational zones: sub-rated ($V_{cut-in} \leq V_w < V_{rated}$) and rated-to-cut-off ($V_{rated} \leq V_w \leq V_{cut-off}$) speed regions [8]. Three MPPT methods are presented: a traditional OTC and a fuzzy logic intelligent control algorithm (type 1 and type 2). The focus is on the installation of a IT2FLC in comparison with a T1FLC.

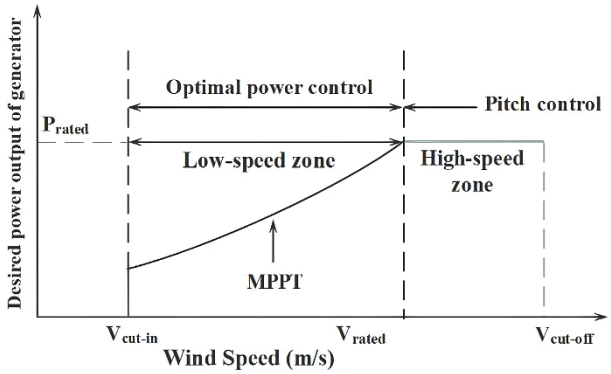

Figure 2. Desired performance level curve of the generator

3.1. Classical optimal torque control

The target of WES is to harness as much energy from the wind as possible in the shortest amount of time [30]. Various MPPT techniques can help to accomplish this. In the OTC method [8], [31], the reference torque T^*_{em} is determined by measuring the mechanical speed of a wind generator ω_m, which is described as (17).

$$T^*_{em} = 0.5 \frac{\rho \pi R^2}{\lambda^3_{opt} G^3} C_p^{max} \omega_m^2 \quad (17)$$

OTC is commonly used for its simplicity and easy-to-implement approach. While this controller is effective under near-optimal operating points, its performance is not optimal under both dynamic wind and the nonlinearities of the WECS.

3.2. Fuzzy logic controller design for MPPT

In this paper, the effectiveness of T2FLCs for the maximum power extraction from DFIG-based WECS is explored in detail in terms of different wind conditions and variable system parameters. Compared with classical T1FLCs with crisp membership functions (MF), T2FLCs with fuzzy MF are well suited to address environmental inexactness, modeling uncertainty, and measurement disturbance [23]. The T2FLC's extra type-reduction method will further enhance decision accuracy in very nonlinear WECS [21]. More precisely, the footprint of uncertainty (FOU) plays an important role in capturing the interval uncertainty in T2FLCs, which reflects the span of all possible membership grades due to uncertainties of system parameters, measurement noise, or model error. To account for this uncertainty, type-reduction generally carries out the conversion of the type-2 fuzzy set to a type-1 fuzzy set such that defuzzification can be applied. For type reduction, the Karnik–Mendel algorithm is the most popular method to calculate the FOU centroid effectively [20]. However, the computational complexity of meet and join operations is still a problem for some practical systems in both the rule generation stage and the classification stage, even though many improved algorithms have been developed for them.

As illustrated in Figure 3, a standard fuzzy logic controller (FLC) comprises a fuzzifier, inference engine, and defuzzifier. The Mamdani inference is chosen because of its low computational burden and has been successfully used in control applications [21], as depicted in Figure 4. This controller is fed by two variables, change in mechanical speed ($\Delta\Omega_m$) and change in mechanical power (ΔP_m), and generates the optimal reference rotor speed (Ω^*_{FLC}). The "Perturb and Observe"-like approach, but using fuzzy logic to determine the magnitude and direction of the next perturbation. The input values ($\Delta\Omega_m$, ΔP_m) are fuzzified using triangular symmetrical MF (Figures 5 and 6) trained to achieve effective MPP tracking, with linguistic labels: NB → negative big, NM → negative medium, NS → negative small, Z → zero, PS → positive small, PM → positive medium, and PB → positive big. its inference rules (shown in Table 1) calculate the changes in the rotor speed and are defuzzified using the centroid-of-area to define the decision output.

Table 1. Decision rules of the interval type-2 and type-1 fuzzy logic controllers (IT2FLC and T1FLC)

$\Delta\Omega_m$	ΔP_m						
	NB	NM	NS	Z	PS	PM	PB
N	PB	PM	PS	NS	NS	NM	NB
Z	NM	NS	NS	Z	PS	PS	PM
P	NB	NM	NS	PS	PS	PM	PB

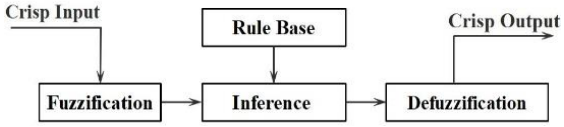

Figure 3. The structure of the FLC

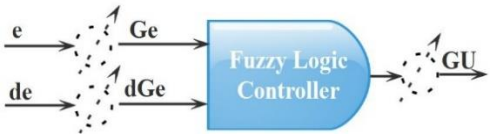

Figure 4. Basic scheme of an FLC: parameters Ge, dGe, and Gu define the fuzzy controller's adaptation

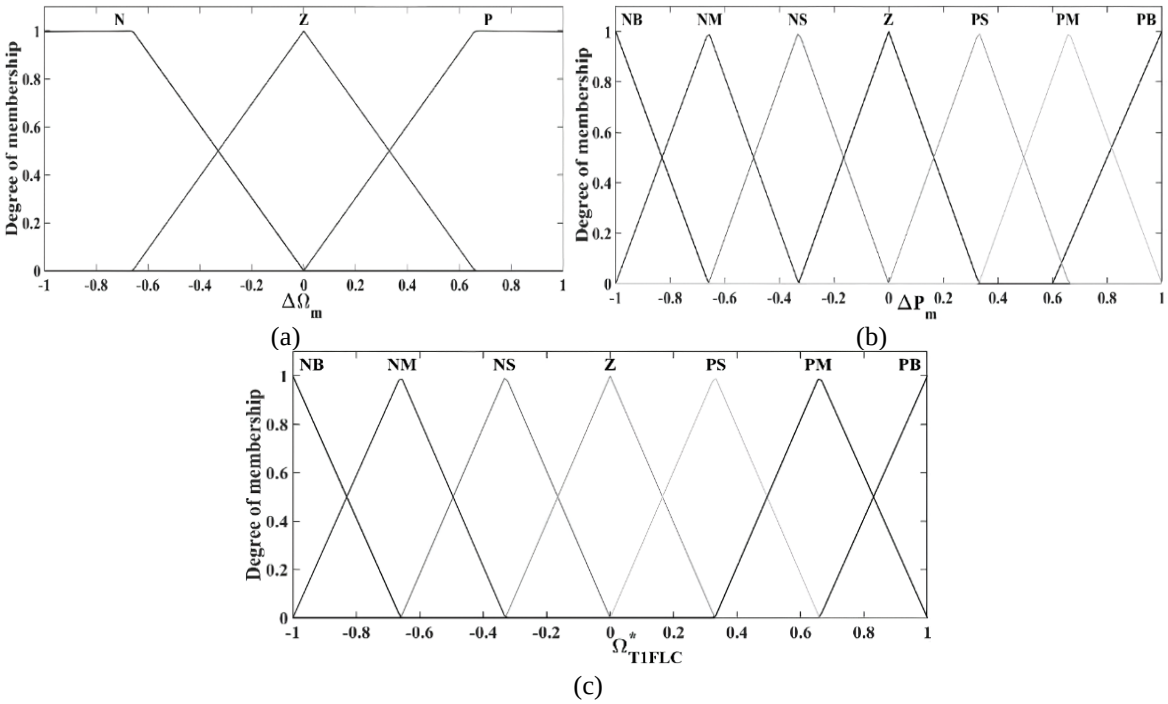

Figure 5. Membership functions of the input and output variables in the proposed type-1 FLC, from left to right: (a) rotor speed, (b) mechanical power, and (c) control output

3.3. Implementation of type-1 and type-2 FLCs

Both T1FLC and IT2FLC have the same architecture, as depicted in Figure 7, but they manage uncertainty in a different manner. The controller in these studies perturbs the rotor speed reference ($\Delta\omega_m$) and observes the accompanying change in power (ΔP_m) in order to iteratively track the maximum power point. If power increases with increasing rotor speed, the search is continued in the same direction; otherwise, it is continued in the opposite direction. This adaptive mechanism provides efficient MPP tracking across varying wind speed conditions and system dynamics.

Control performance is studied by simulating under the real wind profile and then investigating the MPPT under fast wind variation and system uncertainty. Quantitative analysis [24] employs the well-known statistical measures, such as root mean square error (RMSE), the mean absolute error (MAE), and the root-mean-square (RMS) deviation of power tracking (P_e). These are performance evaluation parameters, which stand for reference units to evaluate the responsiveness of the proposed intelligent controllers in tracking maximum power from WECS.

$$e_{T1} = x_t - x_{T1}^* \quad (18)$$

$$e_{T2} = x_t - x_{T2}^* \quad (19)$$

Where $x_t = \Omega_m \; and \;\; x_T^* = \Omega_{T1FLC}^* \; or \; \Omega_{T2FLC}^*$

$$RMSE = \sqrt{\frac{1}{N}\sum_{t=1}^{N}(x_t - x_t{}^*)^2} \quad (20)$$

$$MAE = \frac{1}{N}\sum_{t=1}^{N}|x_t - x_t^*| \quad (21)$$

$$RMS(P_e) = \sqrt{\frac{1}{N}\sum_{t=1}^{N}|P_t|^2} \quad (22)$$

Thereafter, assessing the efficacy ε_{MPPT} of intelligent approaches which are calculated mathematically as (23) [11], [29].

$$\varepsilon_{MPPT} = \frac{\int_0^{tf} P_e dt}{\int_0^{tf} P_{max}} \quad (23)$$

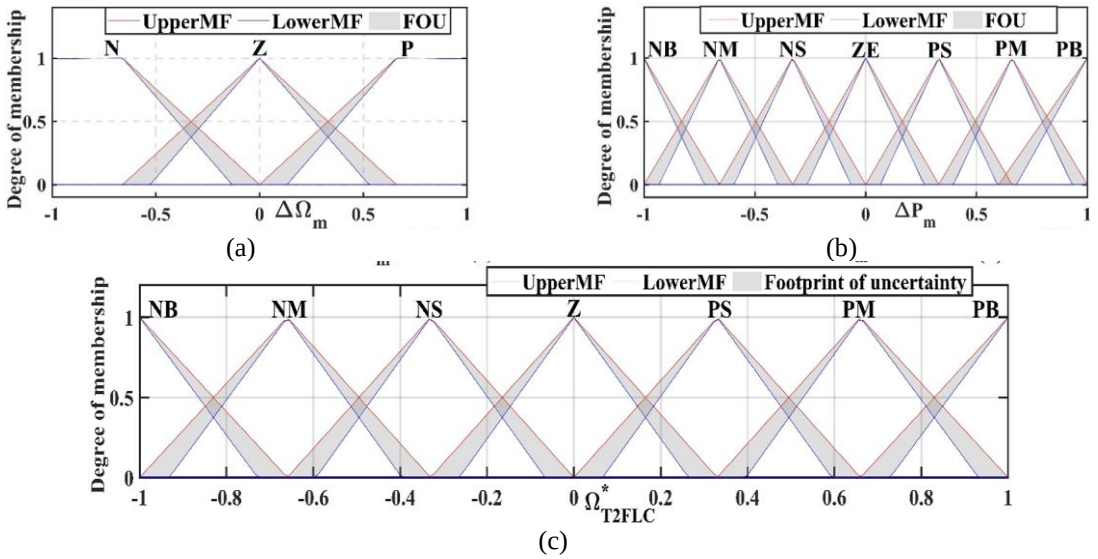

Figure 6. Membership functions of the input and output variables in the proposed type-2 FLC, from left to right: (a) rotor speed, (b) mechanical power, and (c) control output

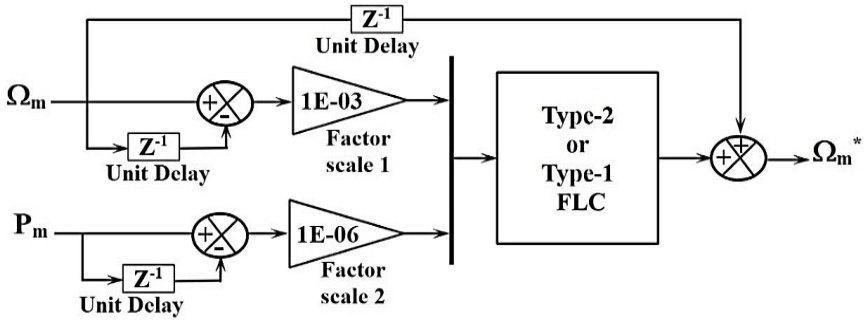

Figure 7. Proposed control scheme employing interval type-2 and type-1 FLCs for MPPT in the WECS

4. RESULTS AND DISCUSSION

This section discusses the comprehensive evaluation of the performance of the WECS–DFIG controlled by the IT2FLC, OTC, and T1FLC depicted in Figure 8. The wind speed profile as a function of time in Figure 9 accounts for the effects of possible uncertainties in the model, such as oscillations in reduced and over turbine inertia, resistances, and inductances. Table 2 outlines the essential parameters of the WT used for simulating the system. To simplify, the system works at a unity power factor while the stator reactive power reference Q_s^* is fixed to zero. The used wind profile is below the rated speed ($V_w < V_{rated}$), which ensures the wind turbine works in the regulation MPPT zone (Figure 2).

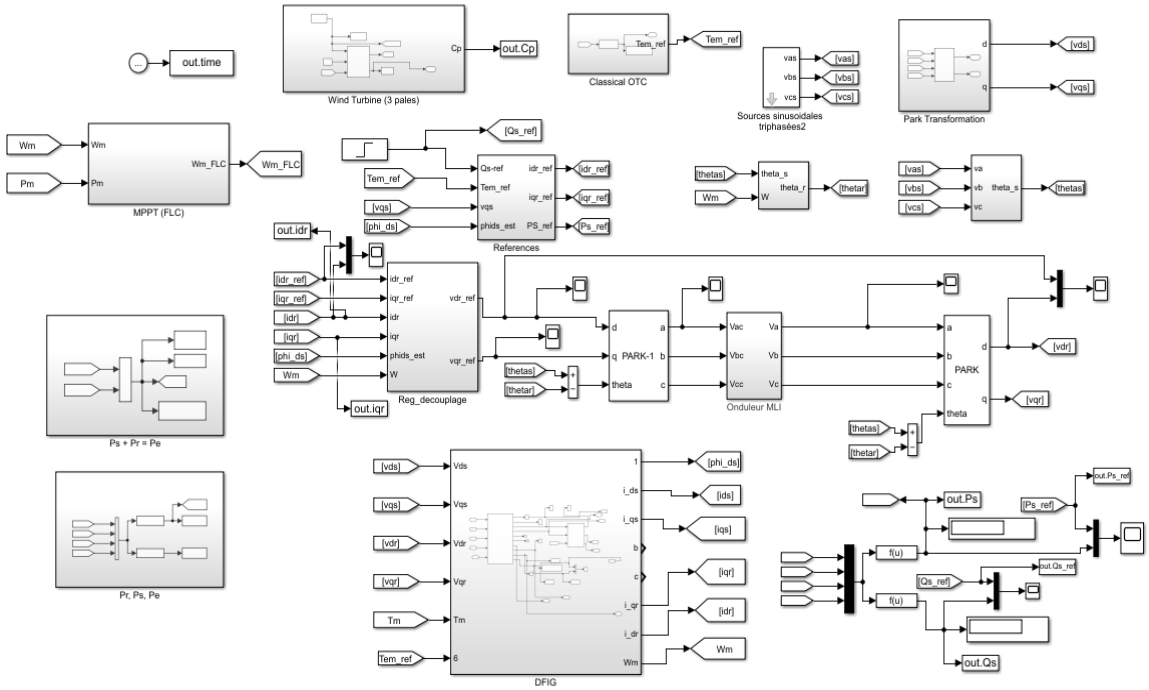

Figure 8. Simulation schematic of the simplified WECS model incorporating a DFIG-based WT

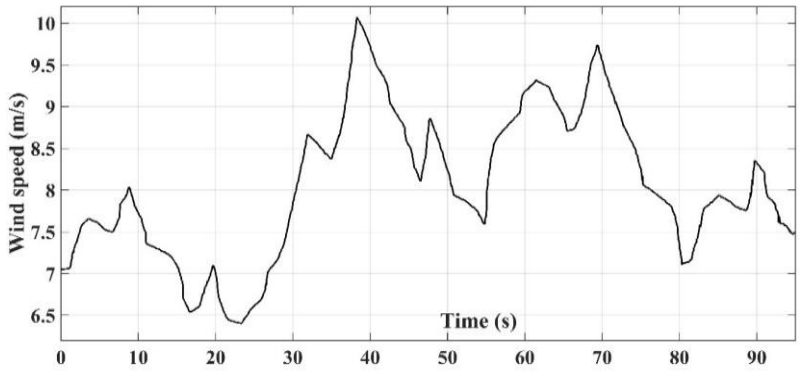

Figure 9. Profile of real wind speed [22]

Table 2. Parameters of the wind turbine system

Symbol	Name	Value/unit	Symbol	Name	Value/unit
Pr	Rated power	1.5 MW	G	Gearbox ratio	100
J	Rotor inertia	1.14 kg.m^2	p	Number of pole pairs	2
Rs	Stator resistance	2.97 mΩ	ρ	Air density	1.225 kg/m^3
Rr	Rotor resistance	3.8 mΩ	R	Rotor radius	90 m
Ls	Stator inductance	12.2 μH	B	Viscous friction	0.1 N.m.s/rad
Lr	Rotor inductance	12.2 μH	f	Grid frequency	50 Hz
M	Magnetization inductance	12.1 μH			

4.1. Rotor speed and torque tracking

Figures 10(a) and 10(b) show the mechanical speed responses of T1FLC and IT2FLC, respectively. In each of the cases studied, the actual velocity follows the reference closely, even if the inertia of the wind generator is strong. Figures 10(c) and 10(d) present the corresponding electromagnetic torque and its reference, indicating good transient and steady-state tracking performances. The torque rises linearly with wind velocity up to its nominal level. Conversion from sub-synchronous to super-synchronous mode is appropriately controlled and smoothly operated over operating ranges as the speed of the rotor approaches a synchronous speed.

4.2. Active and reactive power performance

The active power outputs of the rotor and stator sides, as depicted in Figures 10(e) and 10(f), present results with identical and similar quality performance for the two controllers. Zero reactive power control is also well maintained since the stock current resonant controller is used for operation with a unity power factor. This condition is illustrated in Figures 10(g) and 10(h).

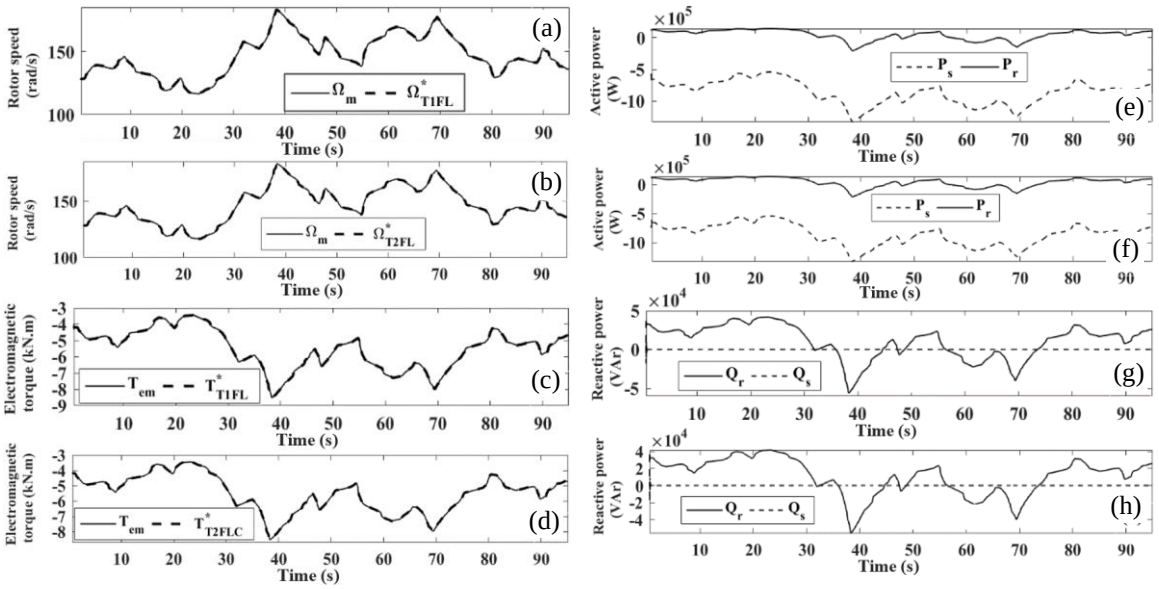

Figure 10. Simulated waveforms of the T1FLC and IT2FLC control schemes for the WECS–DFIG): (a) rotor speed reference, (b) rotor speed measured, (c) electromagnetic torque (d) electromagnetic torque reference, (e) stator active power, (f) rotor active power, (g) stator reactive power, and (h) rotor reactive power

4.3. Robustness under parameter uncertainties

To evaluate robustness, the proposed control schemes (Figure 7) are subjected to ±30% variations in mechanical inertia and ±20 and ±30% uncertainties in electrical parameters, that is:

$$J = 2.54 \pm 30\%, Rr = 0.003 \pm 20\%, Rs = 0.0038 \pm 20\%,$$
$$Ls = 0.012 \pm 30\%, and\ Lr = 0.01 \pm 30\%$$

These parametric uncertainties play an important role in the dynamics of the WECS. For evaluating the dynamic performance of the controller under these kinds of conditions, MATLAB/Simulink environments are used to predict the most important dynamic key parameters of the system, such as MPPT tracking error, rise time, overshoot, settling time, and time to first peak. The relative results under variable wind speed can be seen in Figure 11 and Table 3. Remarkably, the proposed IT2FLC achieves improved tracking precision and also more robustness against parameter changes, which are shown in Figure 12. This enhanced control accuracy is not only to achieve the maximum energy extraction but also to help the predictive maintenance procedure. By regularly checking the controller response, deviations from expected performance can act as an early warning of mechanical wear on the gearbox or generator. Thus, prompt maintenance can be scheduled, and hence the possibility of unscheduled downtime, costly failure, and prolonged operation life of the wind turbine can be reduced.

Table 3. Performance comparison of T2FLC, T1FLC, and OTC under nominal parameters and dynamic wind scenarios

Criteria	Type 2 FLC	Type 1 FLC	OTC
Rise time (s)	0.1856	0.2453	0.0099
Settling time (s)	92.5214	92.5214	59.6870
Settling min (s)	105.2857	108.7065	-9799.2
Settling max (s)	183.3075	183.3071	-0.0822
Overshoot	34.5310	34.5309	249.1811
Peak	183.3075	183.3071	9799.2
Peak time (s)	38.3130	38.3130	51.6433

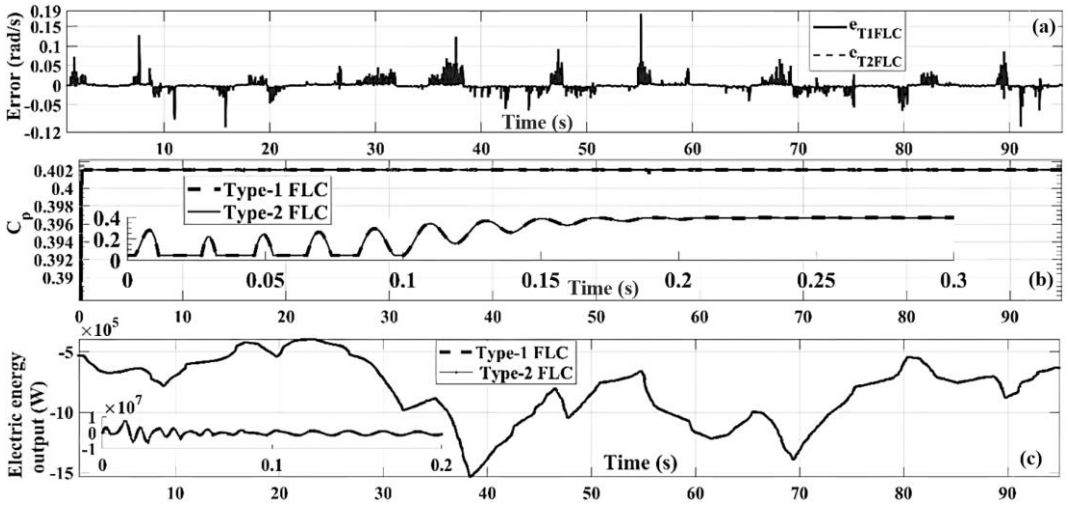

Figure 11. Time-domain comparison of (a) tracking error, (b) power coefficient, and (c) output power using the T1FLC and T2FLC

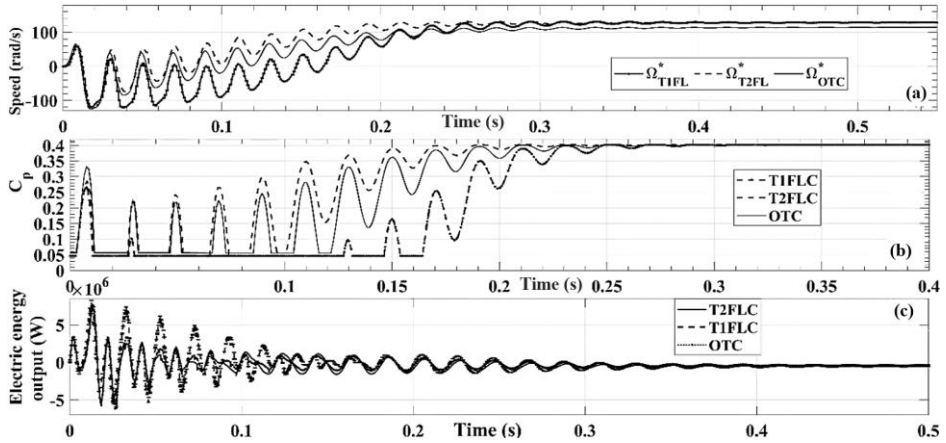

Figure 12. Startup response of the WECS–DFIG under parameter uncertainties and rapid wind speed variations: (a) rotor speed, (b) power coefficient, and (c) generator output power

4.4. Dynamic performance analysis

The most important time-domain performance metrics are listed in Table 3. For instance, using IT2FLC results in a rise time of 0.1856 s, shorter than that for T1FLC (0.2453 s), yet longer compared with classical OTC (0.0099 s). Both fuzzy controllers show similar overshoot (~34.53%) and are much lower than OTC (249.18%). The time to the first peak is also roughly the same for both fuzzy logic schemes (~183.3 s). These numbers tell us that IT2FLC offers more dynamic stability and robustness than the others. Therefore, the better performance of the IT2FLC is due to its capacity to cope with the factors of uncertainties in wind speed and system parameters through the interval MF, which gives a more robust expression of fuzzy sets than the crisp membership functions used in T1FLCs.

4.5. Precision efficiency metrics

Table 4 provides a quantitative comparison of the control schemes implemented performance of the control algorithms by considering the metrics such as MAE, RMSE, and mean squared error (MSE). The much lower MAE and RMSE values of IT2FLC imply its outstanding tracking precision and stability for tracking a moving target. Thus, the T2FLC's ability to handle noise and imprecise sensor readings within its fuzzy sets leads to smoother and more accurate tracking, directly resulting in better metrics. That means more dependable power generation — a key for grid operators fighting to maintain a balance between supply and demand. Greater tracking efficiency also equates to fewer fill-in capacity services; open-cycle, fast-response gas turbines, for example, being operated to balance power swings, result in operational cost savings and lower

carbon emissions. This level of performance is especially important for high turbulence cases, where a robust MPPT is necessary to extract energy efficiently while keeping the mechanical load on the generator as low as possible. Since the IT2FLC can consistently track the MPP trajectory, the overall energy yield increases, as well as mechanical wear decreases, resulting in an increase in the system lifetime.

Furthermore, the energy conversion efficiencies of other control strategies are listed in Table 5. It is concluded that the IT2FLC has the best energy yield of (51.71%) compared to the T1FLC (51.64%) and the classical OTC (32.44%). Based on the robustness analysis in Table 4, the proposed controller can guarantee the robustness under parameter variation and meet the grid code requirement for the power stability of wind turbines during recent wide operating ranges. To conclude, the IT2FLC demonstrates enhanced fault ride-through capabilities, maintaining grid connectivity during transient disturbances such as voltage dips. This feature is essential for improving the reliability and resilience of modern power systems as wind energy integration continues to increase.

Table 4. Comparison of performance indices for T2FLC, T1FLC, and OTC under nominal and dynamic operating conditions

Algorithm	Standard conditions			Under uncertainties		
	MAE	RMSE	RMS	MAE	RMSE	RMS
OTC	1.1775	9.7017	1.4050×10^{6}	1.1295	13.1230	9.1342×10^{5}
T1FLC	2.84	66.18	8.6303×10^{5}	0.093	1.4895	8.7793×10^{5}
T2FLC	2.83	66.15	8.6303×10^{5}	0.0282	0.6587	8.6303×10^{5}

Table 5. Efficiency comparison of MPPT algorithms

Algorithms	Type 1 FLC	Type 2 FLC	OTC
ε(%)	51.6456	51.7128	32.447

4.6. Discussion

The simulation results confirm the robustness and adaptability of the IT2FLC under a large number of parametric uncertainties (inertia and electrical parameters) and a fast-varying wind speed. While both fuzzy logic controllers (T1FLC and IT2FLC) had good MPPT results, the robustness enhancement exhibited by the IT2FLC structure to parameter variations provides a unique advantage for real-time wind farm operation. Technical factors, including fluctuations of voltage, degradation of components, and random gusts of wind affecting system parameters, are highly uncertain. The IT2FLC exhibits high robustness against the above uncertainties and variations, which demonstrates the possibility of using the proposed control in uncertain and variant operational states. This reliability makes IT2FLC a more realistic and resilient method than traditional control methods that can be easily affected by system parameter uncertainties.

Although the IT2FLC performs well, the addition of adaptive controls can further enhance performance. In particular, a real-time adaptive IT2FLC that is able to adjust its parameters using online measurements (e.g., wind speed, grid voltage, and mechanical loading) can enhance system responsiveness and increase energy harvesting capability. In this way, the control strategy can carry on with corresponding optimization to improve with time both the energy harvesting performance and stability of the system when a dynamic variation in it happens. Future research should therefore explore the development and experimental validation of adaptive IT2FLC architectures, with particular emphasis on real-time implementation and performance under grid-connected scenarios.

5. CONCLUSION

This work has developed an improved speed-sensorless maximum power point (MPP) tracking control strategy for variable-speed wind energy conversion systems DFIGs, which combines interval type-2 fuzzy logic (T2FL), type-1 fuzzy logic (T1FL), and OTC. This technique can clearly identify and control rotor rotational speed to optimize for power yield in variable parameters and wind scenarios. The simulation results confirm that the dynamic and steady-state performance of the developed T2FL-based controller is superior to that of the T1FL and OTC models, with lower rise times, settling times, and absolute mean and root-mean-square errors. In addition, the proposed scheme provides fast and stable MPP tracking across a broad operating condition range, such that its robustness to wind speed changes, system inertia change, and different electrical parameters is improved while reducing data dependency as well as power oscillations. Further investigations would look for the potential of implementing into wind systems and the possibility of hybridizing T2FL with adaptive neuro-fuzzy inference systems and bio-inspired optimization methods in order to improve the system stability, adaptability, and efficiency. Further, an adaptive T2FLC could self-tune its membership functions in real-time, enhancing performance under extreme, unforeseen conditions.

FUNDING INFORMATION

The authors state that no funding involved.

AUTHOR CONTRIBUTIONS STATEMENT

This journal uses the Contributor Roles Taxonomy (CRediT) to recognize individual author contributions, reduce authorship disputes, and facilitate collaboration.

Name of Author	C	M	So	Va	Fo	I	R	D	O	E	Vi	Su	P	Fu
Driss Belkhiri	✓	✓	✓	✓	✓	✓		✓	✓	✓				
Boujemaa Nassiri					✓	✓				✓				
Mohamed Ajaamoum		✓				✓		✓	✓	✓	✓	✓	✓	

C : **C**onceptualization
M : **M**ethodology
So : **So**ftware
Va : **Va**lidation
Fo : **Fo**rmal analysis
I : **I**nvestigation
R : **R**esources
D : **D**ata Curation
O : Writing - **O**riginal Draft
E : Writing - Review & **E**diting
Vi : **Vi**sualization
Su : **Su**pervision
P : **P**roject administration
Fu : **Fu**nding acquisition

CONFLICT OF INTEREST STATEMENT

Authors state no conflict of interest.

DATA AVAILABILITY

Data availability is not applicable to this paper as no new data were created or analyzed in this study.

REFERENCES

[1] D. Belkhiri, M. Ajaamoum, F. Outferdine, A. El Idrissi, and E. Boulaoutaq, "Hotspots in hydrogen research and developments: current status, pathways, challenges, and vision to 2050," *e-Prime - Advances in Electrical Engineering, Electronics and Energy*, vol. 13, p. 101089, Sep. 2025, doi: 10.1016/j.prime.2025.101089.

[2] N.-M. Peralta-Vasconez, L. Peña-Pupo, P.-A. Buestán-Andrade, J. R. Nuñez-Alvarez, and H. Martínez-García, "Proposal of a hybrid neuro-fuzzy-based controller to optimize the energy efficiency of a wind turbine," *Sustainability*, vol. 17, no. 8, p. 3742, Apr. 2025, doi: 10.3390/su17083742.

[3] S. A. Eisa, "Modeling dynamics and control of type-3 DFIG wind turbines: stability, Q Droop function, control limits and extreme scenarios simulation," *Electric Power Systems Research*, vol. 166, pp. 29–42, Jan. 2019, doi: 10.1016/j.epsr.2018.09.018.

[4] F. Ullah *et al.*, "A comprehensive review of wind power integration and energy storage technologies for modern grid frequency regulation," *Heliyon*, vol. 10, no. 9, p. e30466, May 2024, doi: 10.1016/j.heliyon.2024.e30466.

[5] A. Kasbi and A. Rahali, "Performance optimization of doubly-fed induction generator (DFIG) equipped variable-speed wind energy turbines by using three-level converter with adaptive fuzzy PI control system," *Materials Today: Proceedings*, vol. 47, pp. 2648–2656, 2021, doi: 10.1016/j.matpr.2021.05.406.

[6] M. Yessef *et al.*, "Optimizing wind energy conversion system efficiency using advanced modified super-twisting direct power control: Real-time implementation on dSPACE 1104 board," *Unconventional Resources*, vol. 8, p. 100224, Oct. 2025, doi: 10.1016/j.uncres.2025.100224.

[7] D. Belkhiri, L. Elmahni, and M. R. El Moutawakil Alaoui, "Intelligent controller for maximum power extraction of wind generation systems using ANN," *International Journal of Nonlinear Sciences and Numerical Simulation*, vol. 24, no. 8, pp. 3023–3038, Jan. 2024, doi: 10.1515/ijnsns-2021-0198.

[8] B. Desalegn, D. Gebeyehu, and B. Tamrat, "Wind energy conversion technologies and engineering approaches to enhancing wind power generation: A review," *Heliyon*, vol. 8, no. 11, p. e11263, Nov. 2022, doi: 10.1016/j.heliyon.2022.e11263.

[9] D. Belkhiri and M. R. E. M. Alaoui, "Improved tracking of optimal torque by artificial neural network for wind energy systems," *International Review on Modelling and Simulations (IREMOS)*, vol. 14, no. 2, p. 110, Apr. 2021, doi: 10.15866/iremos.v14i2.19157.

[10] D. Kumar and K. Chatterjee, "A review of conventional and advanced MPPT algorithms for wind energy systems," *Renewable and Sustainable Energy Reviews*, vol. 55, pp. 957–970, Mar. 2016, doi: 10.1016/j.rser.2015.11.013.

[11] R. Kot, M. Rolak, and M. Malinowski, "Comparison of maximum peak power tracking algorithms for a small wind turbine," *Mathematics and Computers in Simulation*, vol. 91, pp. 29–40, May 2013, doi: 10.1016/j.matcom.2013.03.010.

[12] A. Stetco *et al.*, "Machine learning methods for wind turbine condition monitoring: A review," *Renewable Energy*, vol. 133, pp. 620–635, Apr. 2019, doi: 10.1016/j.renene.2018.10.047.

[13] B. Driss, S. Farhat, K. Abdelilah, and E. M. A. M. Rachid, "Adaptive control for variable-speed wind generation systems using advanced RBF Neural Network," in *2020 1st International Conference on Innovative Research in Applied Science, Engineering and Technology (IRASET)*, Apr. 2020, pp. 1–5. doi: 10.1109/IRASET48871.2020.9092153.

[14] A. P. Marugán, F. P. G. Márquez, J. M. P. Perez, and D. Ruiz-Hernández, "A survey of artificial neural network in wind energy systems," *Applied Energy*, vol. 228, pp. 1822–1836, Oct. 2018, doi: 10.1016/j.apenergy.2018.07.084.

[15] A. O. Baba, G. Liu, and X. Chen, "Classification and evaluation review of maximum power point tracking methods," *Sustainable Futures*, vol. 2, p. 100020, 2020, doi: 10.1016/j.sftr.2020.100020.

[16] M. E. El Telbany, A. Youssef, and A. A. Zekry, "Intelligent techniques for MPPT control in photovoltaic systems: a comprehensive review," in *2014 4th International Conference on Artificial Intelligence with Applications in Engineering and Technology*, Dec. 2014, pp. 17–22. doi: 10.1109/ICAIET.2014.13.

[17] M. S. Mahmoud and M. O. Oyedeji, "Adaptive and predictive control strategies for wind turbine systems: a survey," *IEEE/CAA Journal of Automatica Sinica*, vol. 6, no. 2, pp. 364–378, Mar. 2019, doi: 10.1109/JAS.2019.1911375.
[18] D. A. Umar *et al.*, "Evaluating the efficacy of intelligent methods for maximum power point tracking in wind energy harvesting systems," *Processes*, vol. 11, no. 5, p. 1420, May 2023, doi: 10.3390/pr11051420.
[19] A. Gupta and S. Srivastava, "Comparative analysis of ant colony and particle swarm optimization algorithms for distance optimization," *Procedia Computer Science*, vol. 173, pp. 245–253, 2020, doi: 10.1016/j.procs.2020.06.029.
[20] K. Mittal, A. Jain, K. S. Vaisla, O. Castillo, and J. Kacprzyk, "A comprehensive review on type 2 fuzzy logic applications: past, present and future," *Engineering Applications of Artificial Intelligence*, vol. 95, 2020, doi: 10.1016/j.engappai.2020.103916.
[21] F. Valdez, C. Peraza, and O. Castillo, *General type-2 fuzzy logic in dynamic parameter adaptation for the harmony search algorithm*. Cham: Springer International Publishing, 2020. doi: 10.1007/978-3-030-43950-7.
[22] K. Belmokhtar, M. L. Doumbia, and K. Agbossou, "Novel fuzzy logic based sensorless maximum power point tracking strategy for wind turbine systems driven DFIG (doubly-fed induction generator)," *Energy*, vol. 76, pp. 679–693, Nov. 2014, doi: 10.1016/j.energy.2014.08.066.
[23] A. Medjber, A. Guessoum, H. Belmili, and A. Mellit, "New neural network and fuzzy logic controllers to monitor maximum power for wind energy conversion system," *Energy*, vol. 106, pp. 137–146, Jul. 2016, doi: 10.1016/j.energy.2016.03.026.
[24] A. M. Eltamaly and H. M. Farh, "Maximum power extraction from wind energy system based on fuzzy logic control," *Electric Power Systems Research*, vol. 97, pp. 144–150, Apr. 2013, doi: 10.1016/j.epsr.2013.01.001.
[25] S. Karthikeyan and C. Ramakrishnan, "A hybrid fuzzy logic-based MPPT algorithm for PMSG-based variable speed wind energy conversion system on a smart grid," *Energy Storage and Saving*, vol. 3, no. 4, pp. 295–304, 2024, doi: 10.1016/j.enss.2024.08.001.
[26] S. Velpula and T. Rajaram, "A simple approach to modelling and control of DFIG-based WECS in network reference frame," *International Journal of Ambient Energy*, vol. 43, no. 1, pp. 2475–2485, Dec. 2022, doi: 10.1080/01430750.2020.1740784.
[27] A. A. Salem, N. A. N. Aldin, A. M. Azmy, and W. S. E. Abdellatif, "Implementation and validation of an adaptive fuzzy logic controller for MPPT of PMSG-based wind turbines," *IEEE Access*, vol. 9, pp. 165690–165707, 2021, doi: 10.1109/ACCESS.2021.3134947.
[28] E. S. Abdin and W. Xu, "Control design and dynamic performance analysis of a wind turbine-induction generator unit," *IEEE Transactions on Energy Conversion*, vol. 15, no. 1, pp. 91–96, Mar. 2000, doi: 10.1109/60.849122.
[29] K. Bedoud, M. Ali-rachedi, T. Bahi, R. Lakel, and A. Grid, "Robust control of doubly fed induction generator for wind turbine under sub-synchronous operation mode," *Energy Procedia*, vol. 74, pp. 886–899, Aug. 2015, doi: 10.1016/j.egypro.2015.07.824.
[30] S. Ganjefar, A. A. Ghassemi, and M. M. Ahmadi, "Improving efficiency of two-type maximum power point tracking methods of tip-speed ratio and optimum torque in wind turbine system using a quantum neural network," *Energy*, vol. 67, pp. 444–453, Apr. 2014, doi: 10.1016/j.energy.2014.02.023.
[31] S. He, B. Wang, and Y. Chen, "Improved optimal torque control for large scale floating offshore wind turbines based on interval type-2 fuzzy logic system," *Ocean Engineering*, vol. 330, p. 121186, Jun. 2025, doi: 10.1016/j.oceaneng.2025.121186.
[32] E. H. Mamdani, "Advances in the linguistic synthesis of fuzzy controllers," *International Journal of Man-Machine Studies*, vol. 8, no. 6, pp. 669–678, Nov. 1976, doi: 10.1016/S0020-7373(76)80028-4.

BIOGRAPHIES OF AUTHORS

Driss Belkhiri received his Ph.D. in Electrical Engineering and Renewable Energy from the Higher School of Technology, Ibn Zohr University, Agadir, Morocco. He holds a Bachelor's degree in Experimental Sciences, a Fundamental License in Electronics, and a Master's degree in Radiation and Materials Physics. His research focuses on renewable energy technologies, particularly wind energy systems, green hydrogen production, and control and automation. He integrates artificial intelligence techniques, such as neural networks and fuzzy logic, to enhance energy system performance and efficiency. His doctoral work was carried out at the Laboratory of Engineering Sciences and Energy Management, Agadir, Morocco. He can be contacted at email: driss.belkhiri@edu.uiz.ac.ma.

Boujemaa Nassiri was born in El Jadida, Morocco on January 1, 1974. He received the Master's degree in electronic systems and the Ph.D. degree in medical data processing in 2015 from Ibn Zohr University, Agadir, Morocco. Currently, he received the habilitation degree. His research interests include biomedical signal processing, data processing. He's the head of the Smart Grid and Artificial Intelligence group, Sustainable Innovation and Applied Research Laboratory Within Polytechnique school, International University of Agadir. He can be contacted at email: boujemaa.nassiri@e-polytechnique.ma.

Mohamed Ajaamoum is a professor Ph.D. at the Department of Electrical Engineering, High School of Technology of Agadir, Ibn Zohr University, Agadir, Morocco. His research interests are in photovoltaic systems, fuzzy control, neural networks, renewable energy technologies, system modeling, and power electronics. He can be contacted at email: m.ajaamoum@uiz.ac.ma.